

GEOMETRY AND THE ANOMALOUS HALL EFFECT IN FERROMAGNETS

N. P. ONG and WEI-LI LEE[†]

Department of Physics, Princeton University, New Jersey 08544, U.S.A.

The geometric ideas underlying the Berry phase and the modern viewpoint of Karplus and Luttinger's theory of the anomalous Hall effect are discussed in an elementary way. We briefly review recent Hall and Nernst experiments which support the dominant role of the KL velocity term in ferromagnets.

I. INTRODUCTION

Geometry crops up in physics in unexpected ways. The example in this talk traces an idea proposed 50 years ago. Mired in controversy from the start, it simmered for a long time as an unresolved problem, but has now re-emerged as a topic with modern appeal. In 1954, Karplus and Luttinger (KL) [1] discovered the earliest instance of the Berry phase [3] in solids when they calculated the charge current of electrons moving in a Bravais lattice with broken time-reversal symmetry (a ferromagnet). They uncovered a quantity $\mathbf{\Omega}(\mathbf{k})$ that acts like a "magnetic field" in reciprocal space to produce a transverse velocity $e\mathbf{E} \times \mathbf{\Omega}$. The velocity leads to a dissipationless Hall current which, according to KL, accounts for the anomalous Hall effect (AHE) seen in all ferromagnets [1]. Because Berry-phase physics lay far into the future, the KL theory encountered stiff resistance. From the 60's to late 70's, Smit's rival skew-scattering theory [2] gained ascendancy, with apparent support from experiments on dilute Kondo systems, e.g. CuMn (in hindsight, these experiments are irrelevant because the host lattice retains time-reversal invariance).

In the past 4 years, interest in topological currents derived from the quantum Hall effects has led to the re-examination of the KL theory from the modern viewpoint [4–9]. The new treatments show that KL's early perturbative approach has a much broader generality [4, 5]. Experiments [10–13] show that the Berry phase plays a key role in the Hall effect of magnetic materials. The evidence that the KL theory provides the cor-

rect explanation of the AHE and Nernst effect in ferromagnets is reviewed here.

In a Hall experiment on a ferromagnet, the observed Hall resistivity ρ_{xy} is the sum of the AHE resistivity ρ'_{xy} and the usual Lorentz term R_0H (R_0 is the ordinary Hall coefficient). We have

$$\rho_{xy}(T, H) = R_0(T)H + \rho'_{xy}(T, H). \quad (1)$$

At a fixed T , the strong H dependence of the AHE term simply reflects the rotation of all domains into alignment. This is expressed as $\rho'_{xy}(T, H) = R_s(T)M(T, H)$ where the anomalous Hall coefficient $R_s(T)$ is the scale factor relating the magnetization M to ρ'_{xy} . Our interest is on the value of ρ'_{xy} in the impurity scattering regime.

In this talk, we introduce the geometric ideas underlying the KL theory and review recent experiments. [Readers familiar with holonomy may skip to Sec. IV.]

II. GEOMETRY

Imagine that a beetle moves a unit vector \mathbf{v} along a closed path C on a curved surface (e.g. a latitude on the globe) with the constraint that $\mathbf{v}(t)$ must always lie in the local tangent plane, i.e. $\mathbf{v} \cdot \mathbf{e}_3 = 0$ where \mathbf{e}_3 is the local normal vector (Fig. 1a). Along the path, we impose the further restriction that the direction of \mathbf{v} is perturbed *minimally* (Fig. 1b). Clearly, \mathbf{v} cannot remain absolutely parallel to itself; the next best thing is to ensure that \mathbf{v} never rotates about \mathbf{e}_3 , i.e. any change $d\mathbf{v}$ must be parallel to $\pm\mathbf{e}_3$ (Fig. 1c), viz.

$$\mathbf{e}_3 \times d\mathbf{v} = 0. \quad (2)$$

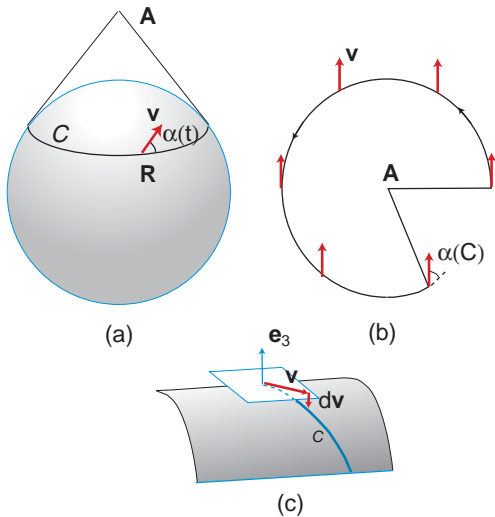


FIG. 1: (a) Transport of \mathbf{v} along the curve C on a sphere. If C is a latitude, the tangent planes are given by the cone with apex A . (b) Flattening the cone on a table shows that \mathbf{v} remains parallel to its initial direction if it is prevented from rotating around the local normal vector \mathbf{e}_3 (parallel transport). However, measured relative to the latitude, \mathbf{v} makes an angle $\alpha(C)$ on returning to the starting point (holonomy). (c) In general, \mathbf{v} lies in the tangent plane (white rectangle). In parallel transport, the change $d\mathbf{v}$ must not have any component in the tangent plane, i.e. $\pm\mathbf{e}_3\|d\mathbf{v}$.

The process satisfying Eq. 2 is known as “parallel transport” (or Levi-Civita transport) [14]. If C is a circle on the sphere, the tangent planes are part of a cone (Fig. 1a). By flattening the cone (Fig. 1b) we see why the no-rotation condition is termed parallel transport. In the “flattened” space, \mathbf{v} is always fixed in direction. However, on the curved surface, the beetle finds that \mathbf{v} does not return to its initial direction when the path is completed. Instead, it makes a “geometric” angle $\alpha(C)$ that is path dependent (holonomy, Fig. 1b).

To measure α , we need a local coordinate frame $[\mathbf{e}_1(t), \mathbf{e}_2(t)]$, where t parametrizes C (on the sphere, these are usually the unit vectors along the latitude and longitude). At each point $\mathbf{R}(t)$, we expand

$$\mathbf{v}(t) = \cos \alpha(t) \mathbf{e}_1(t) + \sin \alpha(t) \mathbf{e}_2(t). \quad (3)$$

As we move along C , the triad $[\mathbf{v}, \mathbf{w}, \mathbf{e}_3]$ (where $\mathbf{w} = \mathbf{e}_3 \times \mathbf{v}$) rotates about the normal by $\alpha(t)$, relative to the local frame $[\mathbf{e}_1, \mathbf{e}_2, \mathbf{e}_3]$. We note that Eq. 2 implies

$$\mathbf{e}_3 \times d\mathbf{w} = 0. \quad (4)$$

Using Eq. 3 in Eq. 2 with the normalization conditions $\mathbf{e}_1 \cdot d\mathbf{e}_1 = 0$ etc, we find the elegant result

$$d\alpha = \mathbf{e}_1 \cdot d\mathbf{e}_2 \equiv \omega_{21}. \quad (5)$$

On completing the trip, the total angle $\alpha(C)$ is the integral of the “connection form” ω_{21} which encodes the overlap between $d\mathbf{e}_2$ and \mathbf{e}_1 [14].

Holonomy seems less mysterious if we regard \mathbf{v} as the quasi-fixed direction relative to which the local frame rotates as we traverse C . This is evident for the flattened cone in Fig. 1b.

These results may be written more compactly using complex vectors with the inner product $(\mathbf{a}, \mathbf{b}) = \mathbf{a}^* \cdot \mathbf{b}$. We write $\hat{\mathbf{n}} = [\mathbf{e}_1 + i\mathbf{e}_2]/\sqrt{2}$ and $\hat{\psi} = [\mathbf{v} + i\mathbf{w}]/\sqrt{2}$. Equation 3 becomes $\hat{\psi}(t) = \hat{\mathbf{n}}(t)e^{-i\alpha(t)}$, with the angle $\alpha(t)$ now appearing as a phase. The parallel transport conditions Eqs. 2, 4 and 5 now have the compact forms

$$\hat{\mathbf{n}}^* \cdot d\hat{\psi} = 0, \quad d\alpha = -\hat{\mathbf{n}}^* \cdot id\hat{\mathbf{n}}. \quad (6)$$

III. BERRY PHASE

In the Berry-phase problem [3] a parameter (the coordinate \mathbf{Q} of the nucleus) is slowly taken around a closed curve C , while the bound electron is assumed to remain in the same eigenstate $|n, \mathbf{Q}\rangle$ parametrized by \mathbf{Q} (Fig. 2a). This assumption is a constraint analogous to that on \mathbf{v} in Sec. II. When the circuit is completed, the electron ket $|\psi\rangle$ does not return to its starting state $|n, \mathbf{Q}_0\rangle$. Instead, it acquires a phase $\chi(C)$ called the Berry phase. We now compare this system with the previous example.

The path C traced by $\mathbf{Q}(t)$ lies on a surface in parameter space \mathbf{Q} . At each \mathbf{Q} , the eigenstate $|n, \mathbf{Q}(t)\rangle$ may be regarded as the local coordinate frame defined in Hilbert

space (in place of the tangent plane), i.e. $|n, \mathbf{Q}(t)\rangle$ is analogous to $\hat{\mathbf{n}}(t)$ in Eq. 6. As C is traversed, the ket of the electron $|\psi\rangle$ is parallel transported, and hence acquires a phase angle relative to $|n, \mathbf{Q}\rangle$, viz. $|\psi\rangle = |n, \mathbf{Q}\rangle e^{-i\chi}$ (Fig. 2b).

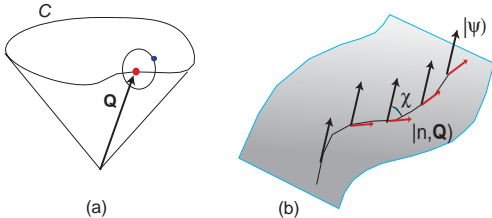


FIG. 2: (a) Electron constrained to same eigenstate $|n, \mathbf{Q}\rangle$ as nuclear coordinate \mathbf{Q} is taken around a closed path C . (b) Parallel transport of ket $|\psi\rangle$ in Hilbert space. As \mathbf{Q} changes, $|\psi\rangle$ acquires a phase angle relative to $|n, \mathbf{Q}\rangle$.

Imposing the parallel-transport condition $\langle n, \mathbf{Q} | \delta |\psi\rangle = 0$ (Eq. 6), we find $\delta\chi = -\langle n, \mathbf{Q} | i\delta |n, \mathbf{Q}\rangle$. On completing the path C , the total Berry phase $\chi(C)$ is the line integral

$$\chi(C) = -\oint_C d\mathbf{Q} \cdot \langle n, \mathbf{Q} | i\nabla_{\mathbf{Q}} |n, \mathbf{Q}\rangle. \quad (7)$$

Physically, as \mathbf{Q} changes, the electronic ket $|\psi\rangle$ stays “parallel” to its initial direction (in the sense of Levi-Civita), while the local reference ket $|n, \mathbf{Q}\rangle$ rotates relative to it. The Berry phase is the phase angle between them.

The form of Eq. 7 suggests that it is fruitful to view the integrand as a (Berry) vector potential $\mathbf{A}(\mathbf{Q}) = \langle n, \mathbf{Q} | i\nabla_{\mathbf{Q}} |n, \mathbf{Q}\rangle$. We may then regard $\chi(C)$ as an Aharonov-Bohm (AB) phase caused by an effective magnetic field $\mathbf{B}(\mathbf{Q}) = \nabla_{\mathbf{Q}} \times \mathbf{A}(\mathbf{Q})$ that lives in parameter space ($\mathbf{B}(\mathbf{Q})$ is called the Berry curvature).

IV. ANOMALOUS VELOCITY

For an electron in a periodic potential, the eigenstates are the Bloch states

$$\psi_{n\mathbf{k}}(\mathbf{r}) = \frac{1}{\sqrt{N}} e^{i\mathbf{k}\cdot\mathbf{r}} u_{n\mathbf{k}}(\mathbf{r}) = \langle \mathbf{r} | n\mathbf{k} \rangle. \quad (8)$$

If we ignore the spin, the band index n and wave-vector \mathbf{k} are sufficient to fully characterize its state.

Let us perturb the electron by adding a static potential $V(\mathbf{r})$. In Bloch representation, the Hamiltonian is

$$H = V(\mathbf{R}) + \epsilon_n(\mathbf{k}), \quad (9)$$

where $\mathbf{R} = i\nabla_{\mathbf{k}}$ is the Wannier coordinate indexing the lattice sites and $\epsilon_n(\mathbf{k})$ is the unperturbed band energy. The potential V causes the wave vector \mathbf{k} to drift along a path C in reciprocal space at the rate

$$\hbar\dot{\mathbf{k}} = -i[\mathbf{k}, H] = -\frac{\partial V}{\partial \mathbf{R}}. \quad (10)$$

In principle, transitions to other bands $n' \neq n$ will occur with finite amplitude. However, for weak V , it is customary to assume that the electron always remains in the same band n . This assumption is a *constraint* analogous to those in the preceding examples. Hence we should expect the electron’s ket vector $|\psi\rangle$ to acquire a Berry phase, i.e. along C , $\langle \mathbf{r} | \psi \rangle = u_{n\mathbf{k}}(\mathbf{r}) e^{-i\chi(\mathbf{k})}$ where

$$\chi(\mathbf{k}) = -\int_C^{\mathbf{k}} d\mathbf{k}' \cdot \mathbf{X}(\mathbf{k}'), \quad (11)$$

with the Berry vector potential $\mathbf{X}(\mathbf{k})$ given by

$$\mathbf{X}(\mathbf{k}) = \int_{cell} d^3r u_{n\mathbf{k}}^*(\mathbf{r}) i\nabla_{\mathbf{k}} u_{n\mathbf{k}}(\mathbf{r}) \quad (12)$$

(\mathbf{X} has dimensions of length). With the substitution $\mathbf{k} \rightarrow \mathbf{Q}$, Fig. 2b equally well depicts the parallel transport of $|\psi\rangle$ as $\mathbf{k}(t)$ changes in reciprocal space.

As in Eq. 7, we may regard χ as the AB phase caused by a magnetic field

$$\mathbf{\Omega}(\mathbf{k}) = \nabla_{\mathbf{k}} \times \mathbf{X}(\mathbf{k}) \quad (13)$$

that lives in \mathbf{k} space.

The Berry curvature $\boldsymbol{\Omega}$ alters the response of the electron to V in an essential way. To see this, we perform a gauge transformation to remove the AB phase at the cost of adding the vector potential \mathbf{X} to $i\nabla_{\mathbf{k}}$ in the argument of V in Eq. 9. The transformed Hamiltonian is then

$$H' = V(i\nabla_{\mathbf{k}} + \mathbf{X}) + \epsilon_n(\mathbf{k}). \quad (14)$$

There are 2 ways to view H' . The role of $\mathbf{X}(\mathbf{k})$ as a vector gauge potential is now manifest. Moreover, in the argument of V , the position operator is now given by

$$\mathbf{x} = \mathbf{R} + \mathbf{X}(\mathbf{k}) \quad (15)$$

instead of just \mathbf{R} . We may view $\mathbf{X}(\mathbf{k})$ as an intracell coordinate that locates the electron within the unit cell. Equation 15 implies that \mathbf{x} fails to commute with itself. Instead we have

$$[x_i, x_j] = i\epsilon^{ijk}\Omega_k. \quad (16)$$

With the Hamiltonian H' , $\hbar\dot{\mathbf{k}}$ is unchanged from Eq. 10, but the group velocity is (using Eq. 16)

$$\hbar\mathbf{v} = -i[\mathbf{x}, H'] = \nabla_{\mathbf{k}}\epsilon_n(\mathbf{k}) + \left(\frac{\partial V}{\partial \mathbf{x}}\right) \times \boldsymbol{\Omega}(\mathbf{k}). \quad (17)$$

The extra term involving $\boldsymbol{\Omega}$ is called the (Luttinger) anomalous velocity.

If $V = -e\mathbf{E} \cdot \mathbf{x}$ (e is the elemental charge and \mathbf{E} an electric field), the semiclassical equations of motion become (we now include a weak, physical magnetic field \mathbf{B} for completeness)

$$\hbar\dot{\mathbf{k}} = e\mathbf{E} + e\mathbf{v} \times \mathbf{B} \quad (18)$$

$$\hbar\mathbf{v} = \nabla_{\mathbf{k}}\epsilon_n - e\mathbf{E} \times \boldsymbol{\Omega}. \quad (19)$$

V. ANOMALOUS HALL CURRENT

In the Boltzmann-equation approach, the charge current density in the absence of \mathbf{B} is

$$\mathbf{J} = e \sum_{\mathbf{k}, s} \mathbf{v}_{\mathbf{k}} [f_{\mathbf{k}}^0 + g_{\mathbf{k}}], \quad (20)$$

where $f_{\mathbf{k}}^0$ is the equilibrium distribution function and $g_{\mathbf{k}} = e\mathbf{v}_{\mathbf{k}}\tau \cdot \mathbf{E}(-\frac{\partial f_{\mathbf{k}}^0}{\partial \epsilon})$ the correction caused by $\mathbf{E}||\hat{\mathbf{x}}$ (τ is the transport relaxation time). Normally, the term in $f_{\mathbf{k}}^0$ sums to zero by symmetry, as it must, leaving the term in $g_{\mathbf{k}}$ to give the usual conductivity σ (the Hall conductivity $\sigma_{xy} = 0$). Now, with $\mathbf{v}_{\mathbf{k}}$ given by Eq. 19, the term in $f_{\mathbf{k}}^0$ yields a sizeable current transverse to \mathbf{E} , viz.

$$\mathbf{J}_H = \frac{e^2}{\hbar} \mathbf{E} \times \sum_{\mathbf{k}, s} \boldsymbol{\Omega}(\mathbf{k}) f_{\mathbf{k}}^0 \quad (21)$$

Because it derives from $f_{\mathbf{k}}^0$, \mathbf{J}_H has the remarkable feature that it is *independent* of τ , as found by KL [1]. We may write the AHE conductivity as

$$\sigma'_{xy} = n \frac{e^2}{\hbar} \langle \Omega \rangle, \quad (22)$$

where $\langle \Omega \rangle \equiv n^{-1} \sum_{\mathbf{k}} \Omega_z(\mathbf{k}) f_{\mathbf{k}}^0$ is the weighted average of the Berry curvature.

Under the time-reversal operation, $\boldsymbol{\Omega}(\mathbf{k}) \rightarrow -\boldsymbol{\Omega}(-\mathbf{k})$, while under inversion, $\boldsymbol{\Omega}(\mathbf{k}) \rightarrow \boldsymbol{\Omega}(-\mathbf{k})$. Hence, if both symmetries are present, $\boldsymbol{\Omega}(\mathbf{k}) = \mathbf{0}$ for all \mathbf{k} . Further, to obtain a finite value in the sum in Eq. 21, we must break time-reversal symmetry (breaking inversion symmetry alone is insufficient). In a ferromagnet, the uniform magnetization \mathbf{M} breaks time-reversal symmetry for the spins. This symmetry-breaking is communicated to the charge currents via spin-orbit coupling. In the simple case of a ferromagnetic semiconductor, Nozieres and Lewiner (NL) [15] have calculated $\mathbf{X}(\mathbf{k}) = -\lambda\mathbf{k} \times \mathbf{S}$, where λ is the spin-orbit coupling parameter and $\mathbf{S} \sim \mathbf{M}$. Equation 21 then gives for the NL model an AHE current $\mathbf{J}_H = 2ne^2\lambda\mathbf{E} \times \mathbf{S}$ that is linear in the carrier density n and \mathbf{M} , but independent of τ .

The quantity that is measured is the Hall resistivity $\rho'_{xy} = \sigma_{xy}\rho^2$. Since $\rho \sim (n\tau)^{-1}$, Eq. 22 immediately implies that [12]

$$\rho'_{xy} = An\rho^2 \quad (23)$$

with ρ the resistivity and $A = e^2\langle \Omega \rangle/\hbar$. In an experiment in which both n and τ can

be varied, the KL theory predicts that ρ'_{xy}/n scales like ρ^α with $\alpha = 2$. By contrast, skew-scattering theories predict $\sigma_{xy} \sim n\tau$ so that ρ'_{xy} is linear in ρ .

VI. SPINEL FERROMAGNET

These predictions have to be tested in the impurity-scattering regime because, if τ is dominated by phonon/magnon scattering, both theories predict $\alpha = 2$. Moreover, it would be desirable to change n greatly (in addition to τ) without destroying the magnetization. These conditions are met in the spinel ferromagnet $\text{CuCr}_2\text{Se}_{4-x}\text{Br}_x$ which is a metal with a Curie temperature $T_C \sim 400$ K (for $x = 0$) [12]. Interaction between the local moments on adjacent Cr ions is ferromagnetic because the Cr–Se–Cr bond is 90° . The holes which reside on the Se bands contribute negligibly to the exchange. Hence tuning the hole density n (by changing the Br content x) hardly affects the magnetization. As x increases from 0 to 1, n decreases from 7×10^{21} to $\sim 10^{20}$ cm^{-3} , while τ decreases by a factor of 70 to give a change in resistivity ρ exceeding 3 decades (measured at 5 K) [12]. However, M at 5 K remains nearly unchanged (T_C decreases to 250 K). Typical profiles of ρ_{xy} vs. H are shown in Fig. 3.

In Fig. 4, $|\rho'_{xy}|/n$ measured in 12 crystals at 5 K is plotted against ρ . As ρ varies over 3 decades, ρ'_{xy}/n increases by 6 decades, following Eq. 23 with $\alpha = 1.95$. This implies that σ'_{xy} is linear in n , but independent of τ . However, the sharp sign change near $x = 0.4$ is not understood at present. [To compare with the skew-scattering prediction, we have also plotted ρ'_{xy} (without dividing by n) against ρ . The data yield an exponent of 1.4 instead of 1. The disagreement with skew scattering lies well outside the uncertainties of the data.]

The experiment provides an estimate of the average Berry curvature $\langle \Omega \rangle$. Using Eq. 22, we find that the parameter $A = 2.24 \times 10^{-25}$ (SI units) gives $\langle \Omega \rangle^{\frac{1}{2}} = 0.30$ Å.

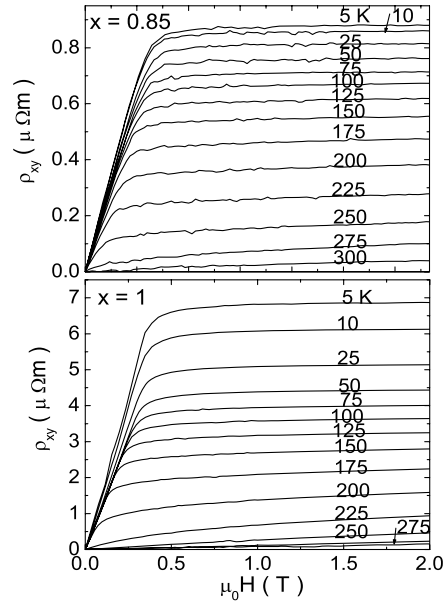


FIG. 3: Traces of the observed ρ_{xy} vs. H in $\text{CuCr}_2\text{Se}_{4-x}\text{Br}_x$ for $x = 0.85$ (top panel) and 1.0 (bottom) [12]. At each T , ρ_{xy} varies like M vs. H (R_0 is negligible). In the $x = 1.0$ sample, ρ'_{xy} at 5 K is possibly the largest AHE resistivity observed to date in a ferromagnet.

VII. ANOMALOUS NERNST EFFECT

The AHE corresponds to a charge current that flows transverse to \mathbf{E} . In addition to the charge, the electron current carries heat. This may be observed by the anomalous Nernst effect [13]. In the Nernst experiment, an applied temperature gradient $-\nabla T || \hat{\mathbf{x}}$ produces a transverse charge current which is antisymmetric in $\mathbf{H} || \hat{\mathbf{z}}$, viz. $J_y = \alpha_{yx}(-\nabla T)$, where α_{ij} is the Peltier conductivity tensor. With the Luttinger velocity, we have

$$\alpha_{xy} = e \sum_{\mathbf{k}, s} \frac{\epsilon_{\mathbf{k}} - \mu}{T} \left(-\frac{\partial f^0}{\partial \epsilon} \right) v_x^0 k_x \Omega_z(\mathbf{k}), \quad (24)$$

where k_B is Boltzmann's constant, μ the chemical potential, and $\hbar \mathbf{v}^0 = \nabla \epsilon(\mathbf{k})$. In deriving this, we have made the substitution $\hbar \mathbf{k} / \tau \rightarrow e \mathbf{E}$ in Eq. 19. Defining the quantity $\langle \Omega \rangle_\epsilon$ as the angular average of $\Omega(\mathbf{k})$ over

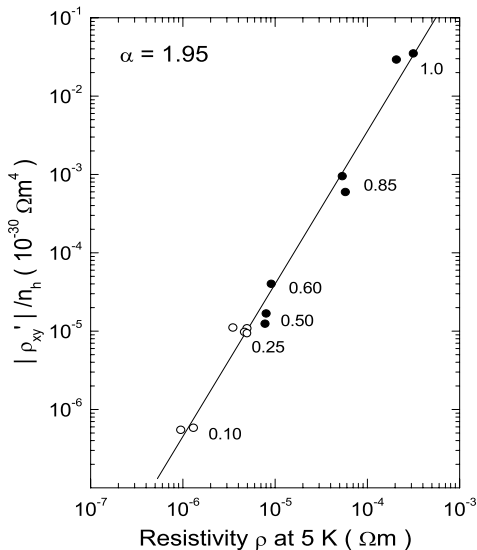


FIG. 4: Plot of the saturation value of ρ'_{xy}/n versus ρ (both measured at 5 K) in log-log scale for 12 crystals of $\text{CuCr}_2\text{Se}_{4-x}\text{Br}_x$ [12]. Open (solid) circles indicate negative (positive) sign for ρ'_{xy} at 5 K (ρ'_{xy} for the $x = 0$ sample is not resolved). The solid line is a fit to $|\rho'_{xy}|/n = A\rho^\alpha$ with $\alpha = 1.95$ and $A = 2.24 \times 10^{-25}$ (SI units).

the Fermi Surface (FS), we may simplify Eq.

24 to

$$\alpha_{xy} \rightarrow \frac{\pi^2}{3} \frac{ek_B^2 T}{\hbar} \frac{2}{3} \left(\frac{\partial \langle \Omega \rangle_\epsilon \mathcal{N}}{\partial \epsilon} \right)_\mu. \quad (25)$$

With the density of states $\mathcal{N} \sim \sqrt{\epsilon}$, the last factor reduces to $\Omega \mathcal{N}_F$ if the ϵ -dependence of Ω is negligible.

In $\text{CuCr}_2\text{Se}_{4-x}\text{Br}_x$, α_{xy} behaves at low T as [13]

$$\alpha_{xy} = \mathcal{A} \frac{ek_B^2 T}{\hbar} \mathcal{N}_F^0 \quad (26)$$

with \mathcal{N}_F^0 the free-electron density of states, and $\mathcal{A} \sim 34 \text{ \AA}^2$. The agreement with Eq. 25 is encouraging although the numerical coefficient seems too large to be simply identified with Ω . We note, however, that the free-electron \mathcal{N}^0 used in Eq. 26 implies that \mathcal{A} is enhanced by the true effective mass. The 2 experiments probe different ways of averaging $\Omega(\mathbf{k})$ over \mathbf{k} .

We acknowledge support from the National Science Foundation (grant DMR 0213706), and helpful comments from F. D. M. Haldane.

[†]Present address of WLL: Johns Hopkins Univ, Dept. Phys. and Astron., Baltimore, MD 21218, USA

-
- [1] R. Karplus, J. M. Luttinger, Phys. Rev. **95**, 1154 (1954); J. M. Luttinger, Phys. Rev. **112**, 739 (1958).
 - [2] J. Smit, Physica (Amsterdam) **21**, 877 (1955); *ibid.* Phys. Rev. B **8**, 2349 (1973).
 - [3] *Geometric Phases in Physics*, ed. Alfred Shapere and Frank Wilczek (World Scientific, 1989).
 - [4] Ganesh Sundaram and Qian Niu, Phys. Rev. B **59**, 14915 (1999).
 - [5] M. Onoda, N. Nagaosa, J. Phys. Soc. Jpn. **71**, 19 (2002).
 - [6] S. Murakami, N. Nagaosa, S. C. Zhang, Science **301**, 1348 (2003).
 - [7] T. Jungwirth, Qian Niu, A. H. MacDonald, Phys. Rev. Lett. **88**, 207208 (2002).
 - [8] Yugui Yao *et al.*, Phys. Rev. Lett. **92**, 037204 (2004).
 - [9] F. D. M. Haldane, Phys. Rev. Lett. **93**, 206602 (2004).
 - [10] P. Matl *et al.*, Phys. Rev. B **57**, 10248 (1998).
 - [11] Y. Taguchi *et al.*, Science **291**, 2573 (2001).
 - [12] Wei-Li Lee, Satoshi Watauchi, V. L. Miller, R. J. Cava and N. P. Ong, Science **303**, 1647 (2004).
 - [13] Wei-Li Lee *et al.*, Phys. Rev. Lett. **93**, 226601 (2004).
 - [14] *Differential Geometry*, J. J. Stoker (Wiley, New York 1969).
 - [15] P. Nozières, C. Lewiner, *J. Phys. (France)* **34**, 901 (1973).